FLUIDELASTIC INSTABILITY IN TUBE ARRAYS

by S. S. Chen, J. A. Jendrzejczyk, and M. W. Wambsganss
Materials and Components Technology Division
Argonne National Laboratory
Argonne, Illinois 60439

Summary

When an array of tubes is subjected to crossflow, the tubes can experience dynamic instability, generally called fluidelastic instability. Instability initiates when the crossflow velocity exceeds a threshold value above which energy input from the flow exceeds that dissipated by system damping. Catastrophic failures of reactor and process plant equipment have been attributed to fluidelastic instability. As a result, extensive research studies have been conducted in the last 15 years with the objective of understanding the instability mechanisms and developing general design guidelines to avoid instability. Argonne National Laboratory has a continuing research program in this area which includes both mathematical model development and experimentation. This paper describes recent developments and accomplishments.

Mathematical models have been developed by various investigators to predict the critical flow velocity at which a given tube array becomes unstable. At present, it is not possible to solve the problem by application of the Navier-Stokes equation and the theory of elasticity. Consequently, various assumptions are made to permit a solution. Because of the limitations imposed by these assumptions, each of these models is only valid in a specific parameter range.

We have developed a general theory for dynamic instability of tube arrays in the form of a unified mathematical model encompassing all of the models proposed by other investigators. The model has already been validated with experimentally determined fluid force coefficient data generated by Tanaka and his colleagues. It has also been used to demonstrate that there are, in fact, two instability mechanisms: fluid-damping-controlled instability and fluid-stiffness-controlled instability. This result facilitates the interpretation of experimental data and the development of associated stability diagrams. The model also provides a tool for use in examining the role of several important nondimensional parameters.

Application of the model requires knowledge of the fluid-force coefficients, in particular, fluid-damping coefficients and fluid-stiffness coefficients. Ideally, these force coefficients can be obtained by experimental, analytical, or numerical techniques. We are currently developing an experimental technique, similar to that employed by Tanaka, that will ultimately allow us to measure the pertinent fluid force coefficients for several tube layout patterns and spacing ratios. Preliminary data are in good agreement with Tanaka's data.

The mathematical modeling is complemented by experimental studies designed to provide additional insights into fundamental phenomena associated with fluidelastic instability, to guide the development of mathematical models, and ultimately to provide a data base for model evaluation/validation. Two of our more recent experimental investigations have involved tube rows in crossflow.

In the first investigation, the vibration of a loosely supported tube, also referred to as tube vibration in a tube-support-plate-inactive (TSP-inactive) mode, was examined. Various phenomena associated with instability in a TSP-inactive mode were demonstrated. Inherent characteristics of the response were noted; among other things, tube alignment relative to the TSP hole is an important parameter.

In the second study, four tube rows, each with a different pitch-to-diameter ratio, were subjected to water crossflow. These tests served to demonstrate a number of salient features of fluidelastic instability. Specifically, the following characteristics were demonstrated: two distinct instability mechanisms, discontinuous jump between the two instability regimes, multiple stable and unstable regions, and excited and intrinsic instability flow velocities. Although for the case of tube rows the two instability mechanisms are clearly separated, in other tube arrays both fluid damping and fluid stiffness may be important simultaneously. Nevertheless, the general instability characteristics for arbitrary tube arrays will not be much different from the basic characteristics demonstrated for tube rows.

Wambsganss

FLUIDELASTIC INSTABILITY IN TUBE ARRAYS

- OBJECTIVES
  - IMPROVE THE UNDERSTANDING OF INSTABILITY PHENOMENA
  - DEVELOP VALIDATED PREDICTION METHODS
- INTEGRATED THEORETICAL/EXPERIMENTAL APPROACH
  - EXPERIMENTAL STUDIES
  - MATHEMATICAL MODEL DEVELOPMENT

INSTABILITY IN TSP-INACTIVE MODE

- DEFINITIONS*
  - TSP-ACTIVE MODE ⇒ 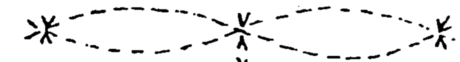
  - TSP-INACTIVE MODE ⇒ 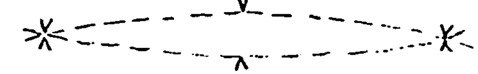
- MOTIVATION
  - PWR SGs (RINGHALS PLANT; U-TUBES)
  - CRBR SG
- POTENTIAL PROBLEM
  - LARGE CLEARANCES (30 TO 40 MILS)
  - SHORT/STIFF SPANS

---

*REF: "DYNAMICS OF TUBES IN FLUID WITH TUBE-BAFFLE INTERACTION," BY S. S. CHEN, J. A. JENDRZEJCZYK, AND M. W. WAMBSGANSS, ASME J. PRESSURE VESSEL TECHNOLOGY, 107, PP. 7-16, 1985.

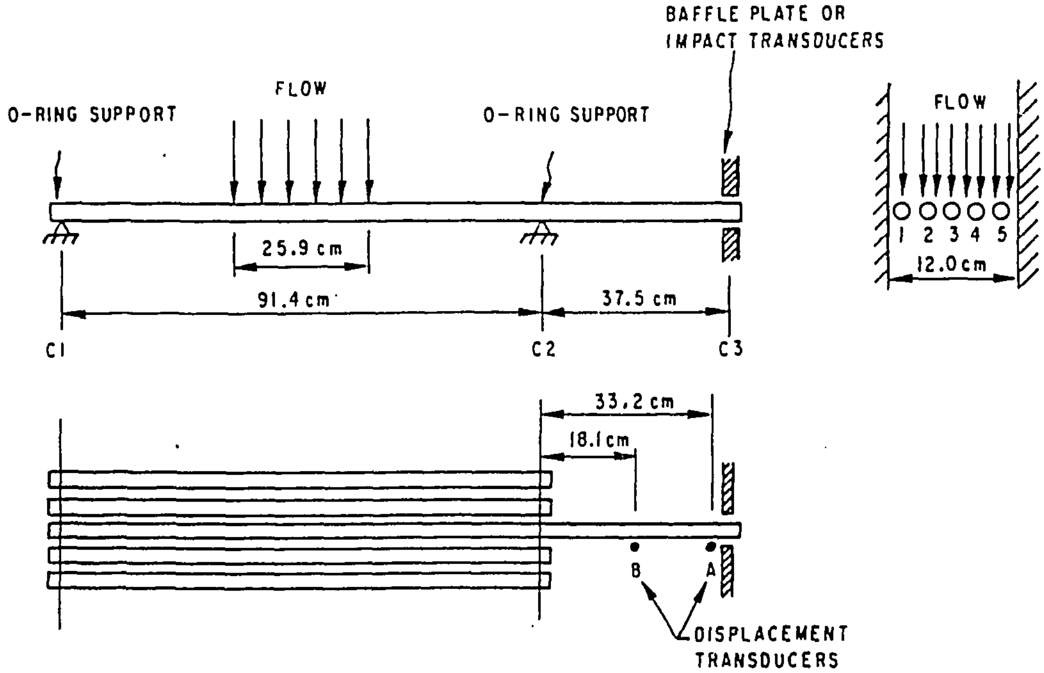

Schematic of a tube row.

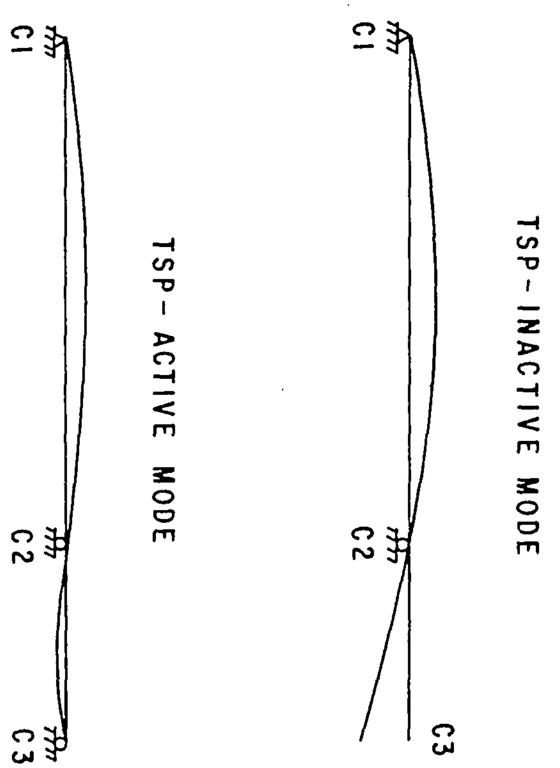

TSP-inactive and TSP-active modes.

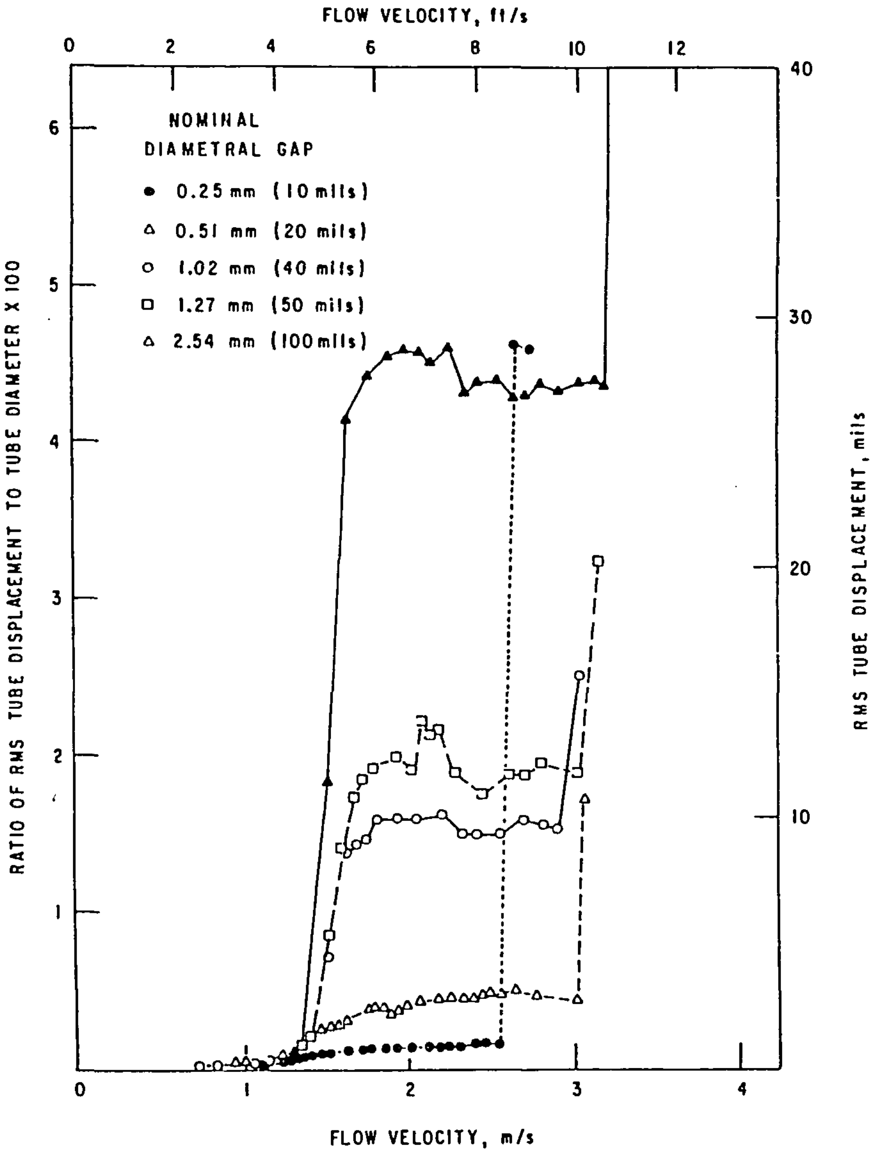

RMS tube displacements as a function of flow velocity for various diametral gaps (Test A1).

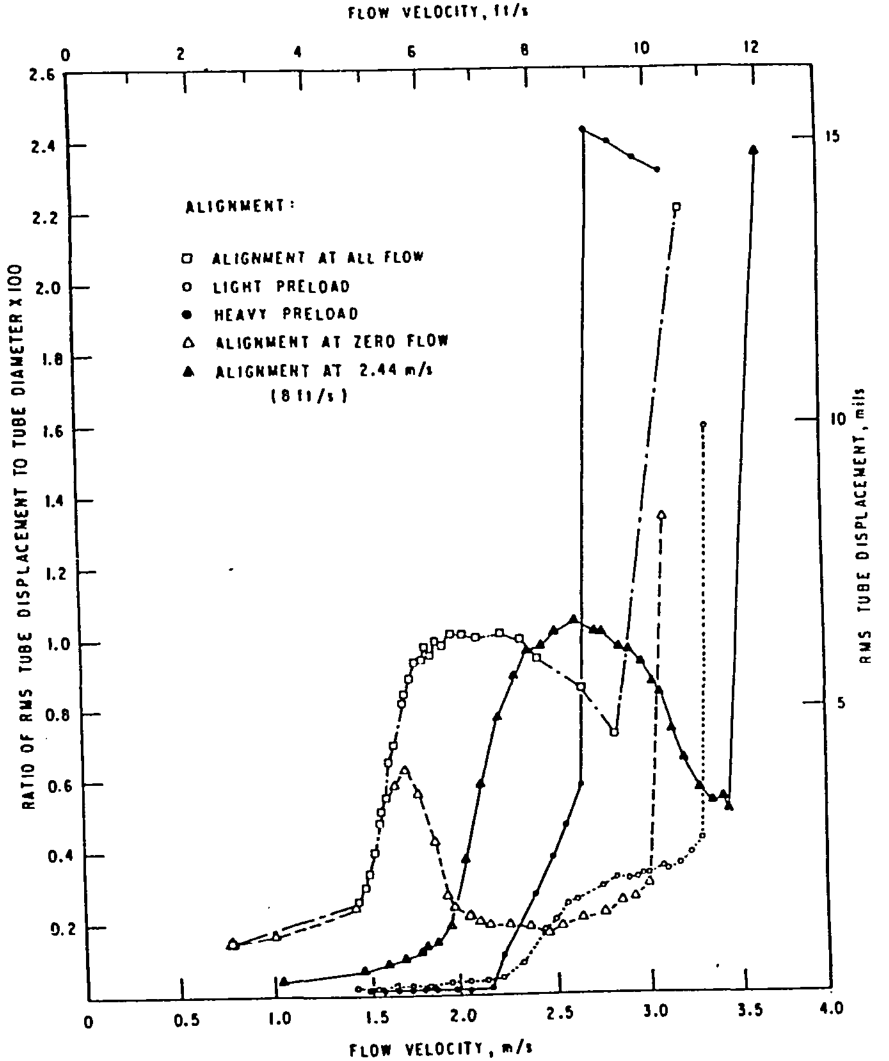

RMS tube displacements as a function of flow velocity for different alignments with a diametral gap of 0.64 mm (Test A1).

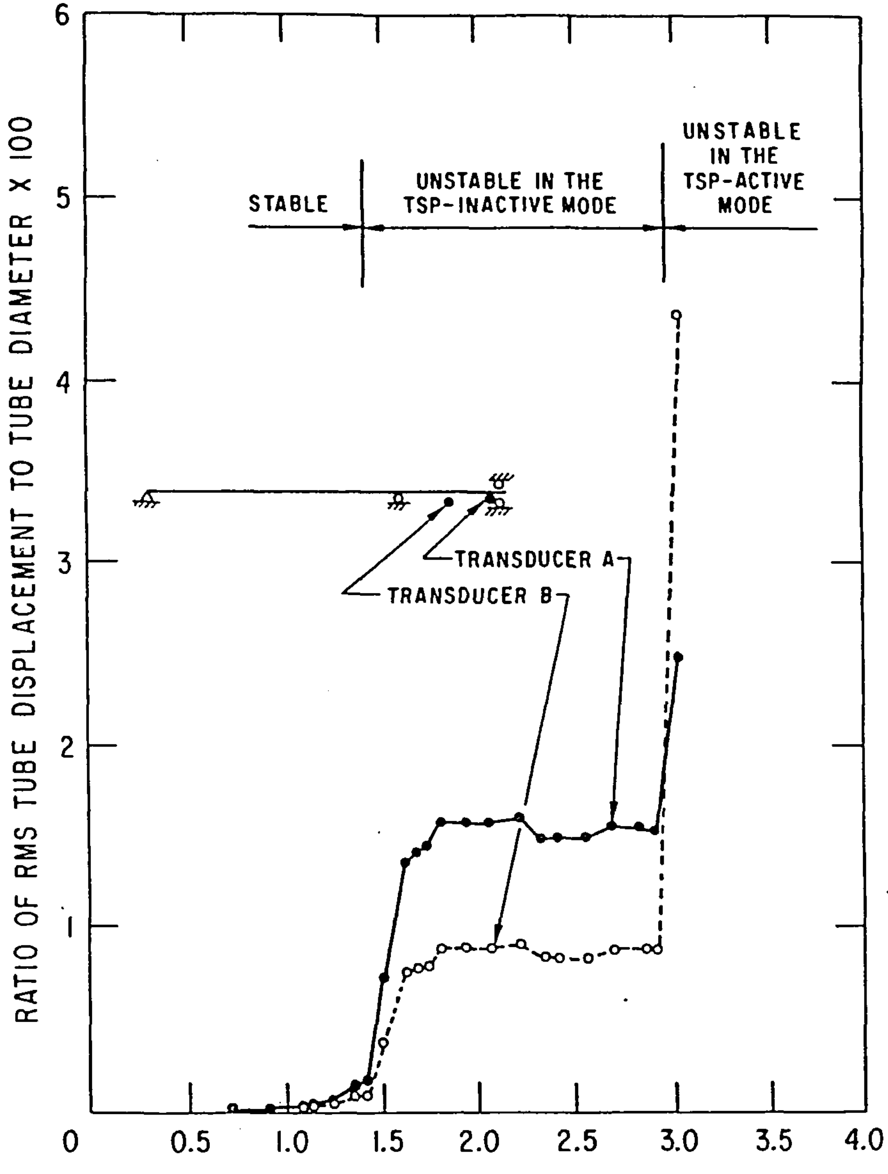

RMS tube displacements as a function of flow velocity for Test A1 with a diametral gap of 1.02 mm.

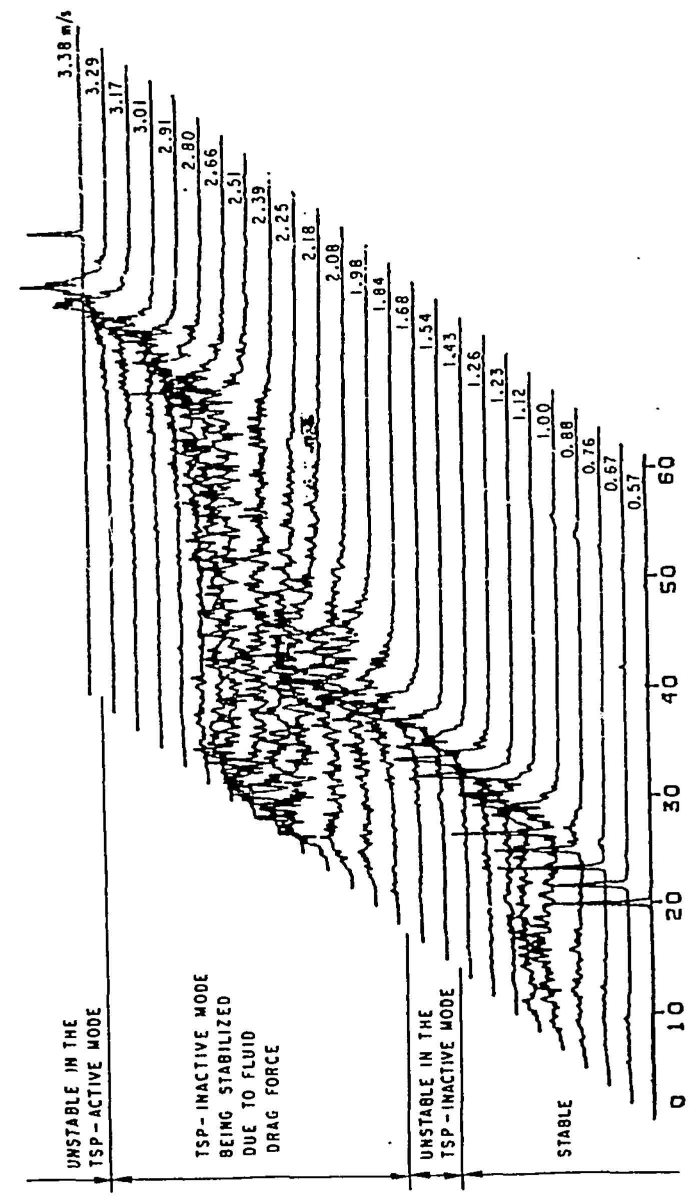

Frequency spectra of tube displacement for the diametral gap equal to 0.64 mm (aligned at zero flow).

SOME RESULTS

- RESPONSE AMPLITUDE LIMITED IN TSP-INACTIVE MODE

- PEAK IMPACT FORCE AND NUMBER OF IMPACTS PER CYCLE INCREASE WITH FLOW VELOCITY AND DIAMETRAL CLEARANCE

- FLUID IN GAP AFFECTS RESPONSE CHARACTERISTICS
  - INCREASES DAMPING ⇒ REDUCES RESPONSE AMPLITUDE
  - INSTABILITY IN TSP-INACTIVE MODE ⇒ REDUCES TUBE DISPLACEMENT AND IMPACT FORCE

- ALIGNMENT IS IMPORTANT PARAMETER
  - DETERMINES RESPONSE IN TSP-INACTIVE MODE
  - MISALIGNMENT CAN BE BENEFICIAL

CONCLUSIONS

- IN HX OR SG POTENTIAL TO VIBRATE IN TSP-INACTIVE MODE DEPENDS ON A NUMBER OF FACTORS -
  - TUBE STRAIGHTNESS
  - TUBE/SUPPORT HOLE TOLERANCES
  - INITIAL MECHANICAL FIT-UP OF TUBES
  - OPERATING CONDITIONS
  - STEADY DRAG AND LIFT FORCES

- DESIGN GUIDANCE -
  - KEEP CLEARANCES SMALL
  - BEWARE OF SHORT/STIFF SPANS

INSTABILITY CHARACTERISTICS OF TUBE ROWS IN CROSSFLOW*

- OBJECTIVES
  - INVESTIGATE "JUMP PHENOMENON" FOR TUBE ROWS AS FUNCTION OF P/D-RATIO
  - INVESTIGATE THRESHOLDS ASSOCIATED WITH "EXCITED" AND "INTRINSIC" INSTABILITIES

- TEST SET-UP
  - 5 TUBE ROW
  - P/D-RATIOS TESTED: 1.35, 1.5, 1.6, 1.75
  - VARIABLE DAMPING
  - MIDDLE THREE TUBES INSTRUMENTED

DEFINITIONS -

- INTRINSIC INSTABILITY -
  - NO EXTERNAL EXCITATION PROVIDED TO TUBES
  - ONCE FLOW VELOCITY REACHES CRITICAL VALUE (V_I) INSTABILITY INITIATES SPONTANEOUSLY

- EXCITED INSTABILITY -
  - THRESHOLD FLOW VELOCITY (V_E) LESS THAN INTRINSIC INSTABILITY THRESHOLD VELOCITY ($V_E < V_I$)
  - FOR $V < V_E$, ANY TUBE MOTION CAUSED BY TRANSIENT DISTURBANCE DIES OUT
  - FOR $V_E < V < V_I$, A TRANSIENT DISTURBANCE MAY INITIATE INSTABILITY

---

*REF: "CHARACTERISTICS OF FLUIDELASTIC INSTABILITY OF TUBE ROWS IN CROSSFLOW," BY S. S. CHEN AND J. A. JENDRZEJCZYK, TO BE PRESENTED AT INT'L CONF. ON FLOW INDUCED VIBRATIONS, BOWNESS-ON-WINDERMERE, ENGLAND, MAY 12-14, 1987

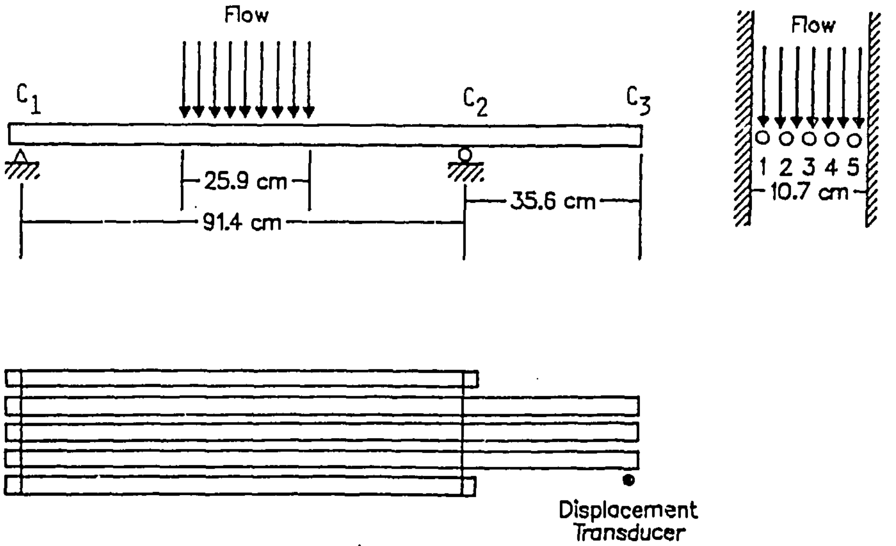

Schematic of Tube Row

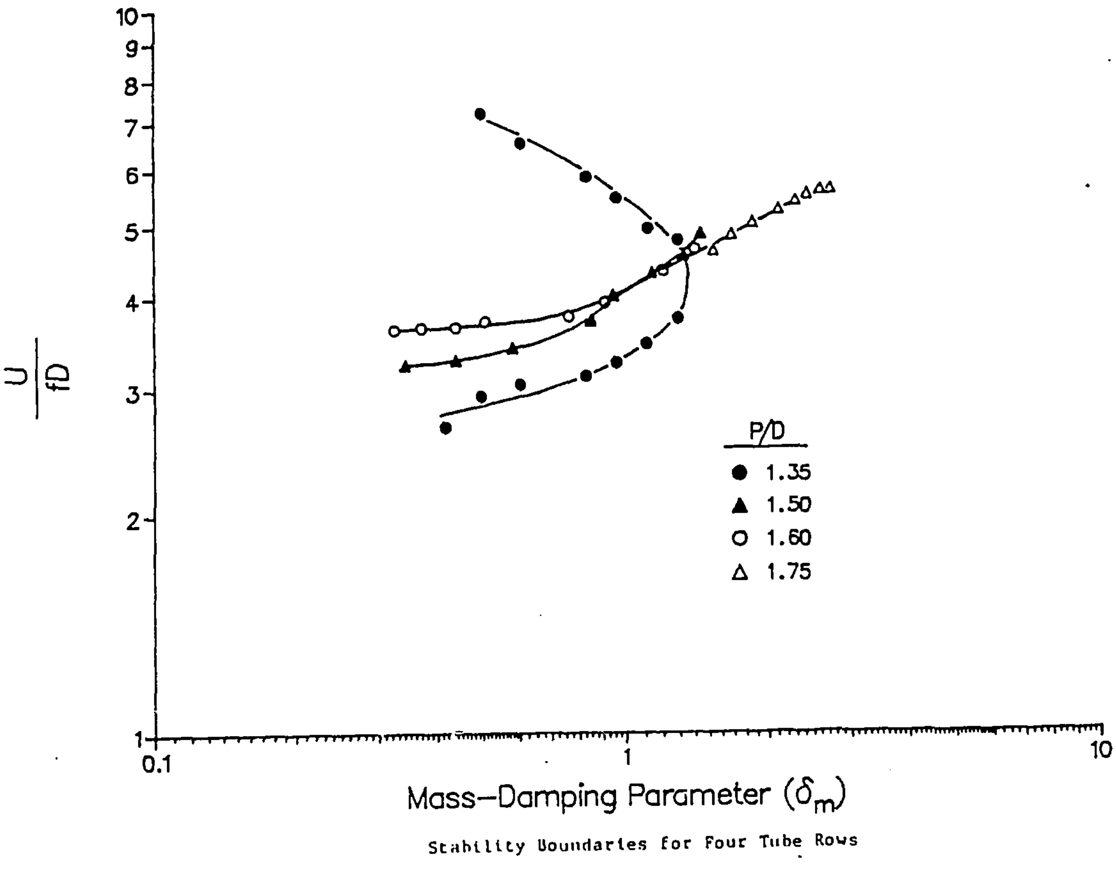

Stability Boundaries for Four Tube Rows

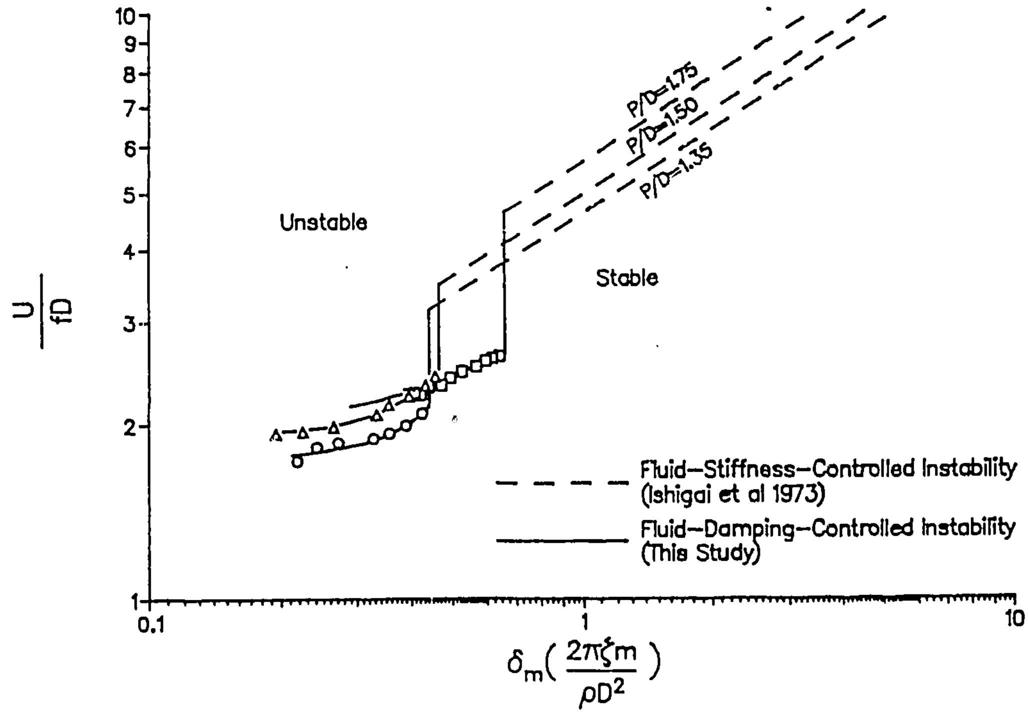

Stability Map for Tube Rows

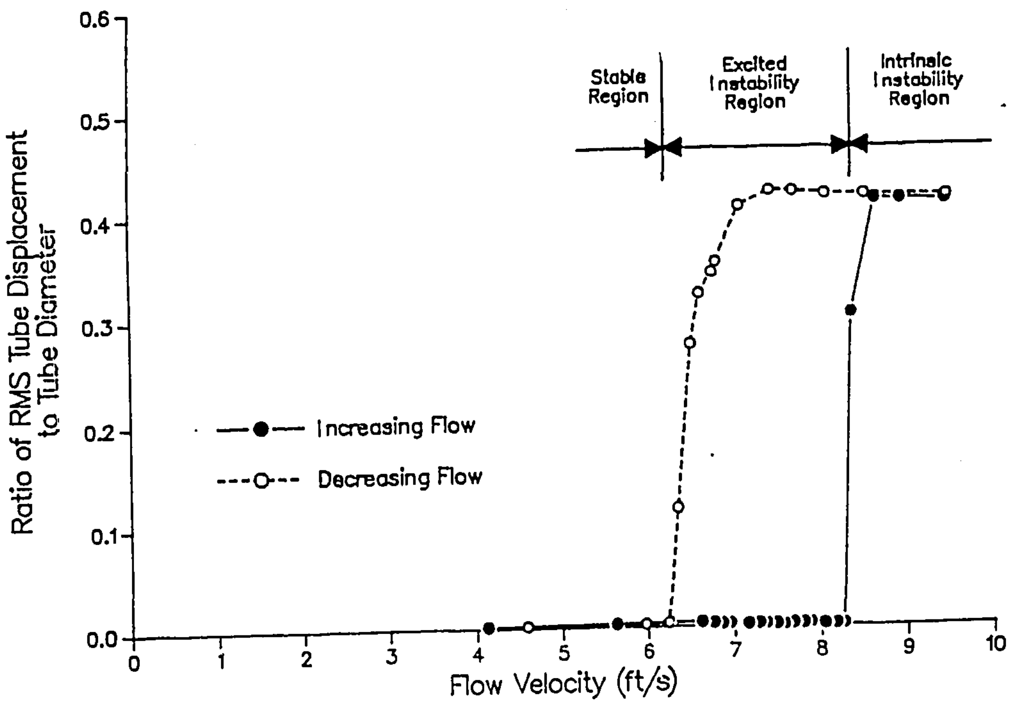

Tube Displacement as a Function of Flow Velocity for P/D = 1.75 at δ_m = 2.15

INSTABILITY CHARACTERISTICS -

- TWO DISTINCT INSTABILITY MECHANISMS
- DISCONTINUOUS JUMP BETWEEN INSTABILITY REGIMES
- MULTIPLE STABLE AND UNSTABLE REGIONS
- AT LOW VALUES OF MASS-DAMPING PARAMETER (δ_m), U_{CR} IS NONLINEAR FUNCTION OF $\delta_m^{0.5}$
- EXCITED INSTABILITY THRESHOLD EXISTS WHICH IS LESS THAN INTRINSIC INSTABILITY THRESHOLD
- HYSTERESIS EFFECT CAN BE STRONG

MATHEMATICAL MODELING

- DEVELOPED GENERAL THEORY FOR DYNAMIC INSTABILITY OF TUBE ARRAYS IN CROSSFLOW
- APPLICATION REQUIRES KNOWLEDGE OF MOTION-DEPENDENT FORCE COEFFICIENTS
  - FLUID STIFFNESS COEFFICIENTS
  - FLUID DAMPING COEFFICIENTS
- TANAKA'S DATA USED TO VERIFY MODEL
- CURRENT EFFORTS ÷ MEASUREMENT OF FORCE COEFFICIENTS
  - FURTHER VALIDATION OF MODEL
  - DATA BASE FOR APPLICATION IN DESIGN EVALUATION

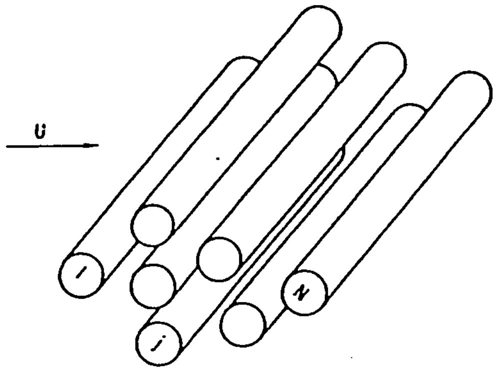

(a) A GROUP OF CIRCULAR CYLINDERS

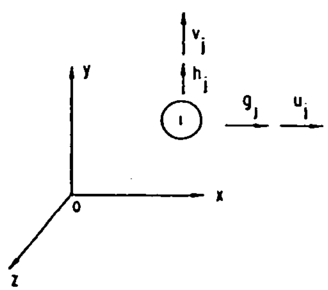

(b) FLUID FORCE AND CYLINDER DISPLACEMENT COMPONENTS

EQUATION OF MOTION FOR CYLINDER j IN x AND y DIRECTIONS ARE, RESPECTIVELY

$$E_jI_j \frac{\partial^4 u_j}{\partial z^4} + C_{sj}\frac{\partial u_j}{\partial t} + m_j \frac{\partial^2 u_j}{\partial t^2} = g_j + g_j', \quad j = 1, 2, 3, \ldots, N,$$

$$E_jI_j \frac{\partial^4 v_j}{\partial z^4} + C_{sj}\frac{\partial v_j}{\partial t} + m_j \frac{\partial^2 v_j}{\partial t^2} = h_j + h_j', \quad j = 1, 2, 3, \ldots, N,$$

Fluid Excitation Forces

$$g_j' = \frac{1}{2}\rho U^2 D C_{Dj} + \frac{1}{2}\rho U^2 D C_{Dj}' \sin(\Omega_{Dj} t + \phi_{Dj}) + g_j'$$

and

$$h_j' = \frac{1}{2}\rho U^2 D C_{Lj} + \frac{1}{2}\rho U^2 D C_{Lj}' \sin(\Omega_{Lj} t + \phi_{Lj}) + h_j',$$

Motion-dependent Fluid Forces

$$g_j = -\sum_{k=1}^{N} \left\{\left[\bar{\alpha}_{jk}\frac{\partial^2 u_k}{\partial t^2} + \bar{\alpha}_{jk}'\frac{\partial u_k}{\partial t} + \bar{\alpha}_{jk}'' u_k\right] + \left[\bar{\sigma}_{jk}\frac{\partial^2 v_k}{\partial t^2} + \bar{\sigma}_{jk}'\frac{\partial v_k}{\partial t} + \bar{\sigma}_{jk}'' v_k\right]\right\}$$

and

$$h_j = -\sum_{k=1}^{N} \left\{\left[\bar{\tau}_{jk}\frac{\partial^2 u_k}{\partial t^2} + \bar{\tau}_{jk}'\frac{\partial u_k}{\partial t} + \bar{\tau}_{jk}'' u_k\right] + \left[\bar{\beta}_{jk}\frac{\partial^2 v_k}{\partial t^2} + \bar{\beta}_{jk}'\frac{\partial v_k}{\partial t} + \bar{\beta}_{jk}'' v_k\right]\right\}.$$

IN TERMS OF DIMENSIONLESS FORCE COEFFICIENTS

$$\bar{\alpha}_{jk} = \rho\pi R^2 \alpha_{jk}\ , \quad \bar{\alpha}'_{jk} = -\frac{\rho U^2}{\omega}\alpha'_{jk}\ , \quad \bar{\alpha}''_{jk} = -\rho U^2 \alpha''_{jk}$$

$$\bar{\sigma}_{jk} = \rho\pi R^2 \sigma_{jk}\ , \quad \bar{\sigma}'_{jk} = -\frac{\rho U^2}{\omega}\sigma'_{jk}\ , \quad \bar{\sigma}''_{jk} = -\rho U^2 \sigma''_{jk}$$

$$\bar{\tau}_{jk} = \rho\pi R^2 \tau_{jk}\ , \quad \bar{\tau}'_{jk} = -\frac{\rho U^2}{\omega}\tau'_{jk}\ , \quad \bar{\tau}''_{jk} = -\rho U^2 \tau''_{jk}$$

$$\bar{\beta}_{jk} = \rho\pi R^2 \beta_{jk}\ , \quad \bar{\beta}'_{jk} = -\frac{\rho U^2}{\omega}\beta'_{jk}\ , \quad \bar{\beta}''_{jk} = -\rho U^2 \beta''_{jk}\ ,$$

MOTION-DEPENDENT FLUID FORCES CAN BE WRITTEN AS

$$g_j = -\rho\pi R^2 \sum_{k=1}^{N}\left(\alpha_{jk}\frac{\partial^2 u_k}{\partial t^2} + \sigma_{jk}\frac{\partial^2 v_k}{\partial t^2}\right) + \frac{\rho U^2}{\omega}\sum_{k=1}^{N}\left(\alpha'_{jk}\frac{\partial u_k}{\partial t^2} + \sigma'_{jk}\frac{\partial v_k}{\partial t}\right) + \rho U^2 \sum_{k=1}^{N}\left(\alpha''_{jk}u_k + \sigma''_{jk}v_k\right)$$

and

$$h_j = -\rho\pi R^2 \sum_{k=1}^{N}\left(\tau_{jk}\frac{\partial^2 u_k}{\partial t^2} + \beta_{jk}\frac{\partial^2 v_k}{\partial t^2}\right) + \frac{\rho U^2}{\omega}\sum_{k=1}^{N}\left(\tau'_{jk}\frac{\partial u_k}{\partial t} + \beta'_{jk}\frac{\partial v_k}{\partial t}\right) + \rho U^2 \sum_{k=1}^{N}\left(\tau''_{jk}u_k + \beta''_{jk}v_k\right) .$$

α_{jk}, σ_{jk}, τ_{jk}, and β_{jk} are called added mass coefficients, α'_{jk}, σ'_{jk}, τ'_{jk} and β'_{jk} are called fluid-damping coefficients, and α''_{jk}, σ''_{jk}, τ''_{jk} and β''_{jk} are called fluid-stiffness coefficients.

MEASUREMENT METHOD - EXAMPLE

EXCITE CYLINDER k IN y DIRECTION, DISPLACEMENT IS GIVEN BY

$$v_k = \tilde{v}_k \exp(i\omega t) \tag{1}$$

FLUID FORCE ACTING ON CYLINDER j IN x DIRECTION IS GIVEN BY

$$g_j = \frac{1}{2}\rho U^2 (c_{jk}\cos\psi_{jk} + i c_{jk}\sin\psi_{jk})\tilde{v}_k \tag{2}$$

WHERE c_{jk} IS FLUID FORCE AMPLITUDE

ϕ_{jk} *IS PHASE ANGLE BETWEEN FORCE AND DISPLACEMENT*

c_{jk} AND ϕ_{jk} ARE MEASURED EXPERIMENTALLY.

FROM UNSTEADY FLOW THEORY WE CAN WRITE

$$g_j = (\rho\pi R^2\omega^2\sigma_{jk} + \rho U^2\sigma''_{jk} + i\rho U^2\sigma'_{jk})\tilde{v}_k \tag{3}$$

COMPARING EQUATIONS (2) AND (3) YIELDS

$$\sigma''_{jk} = \frac{1}{2}c_{jk}\cos\psi_{jk} - \frac{\pi^3}{U_r^2}\sigma_{jk}$$

$$\sigma'_{jk} = \frac{1}{2}c_{jk}\sin\psi_{jk}\ , \tag{4}$$

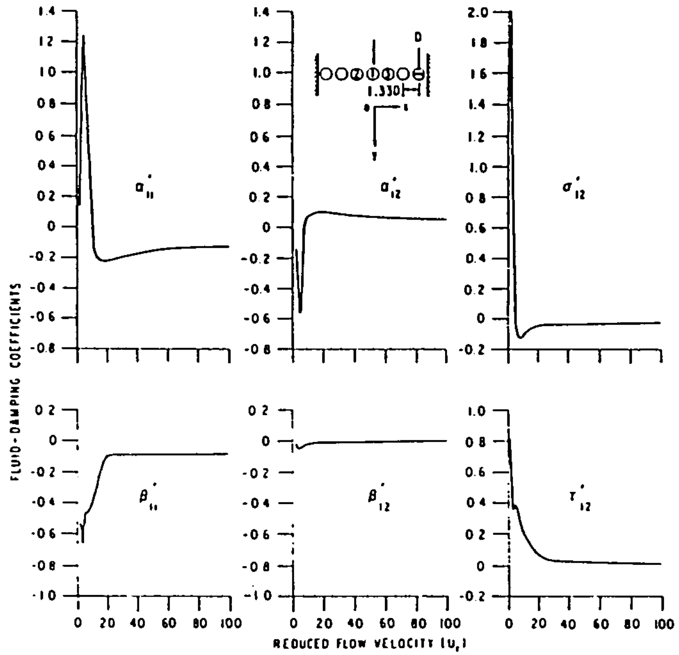

Fluid-Damping Coefficients for a Row of Cylinders

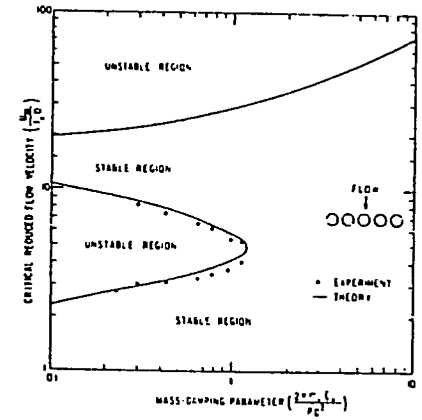

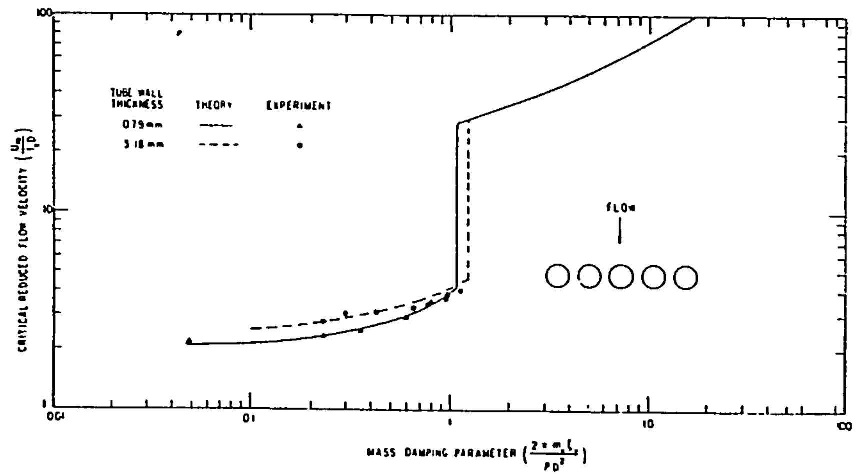

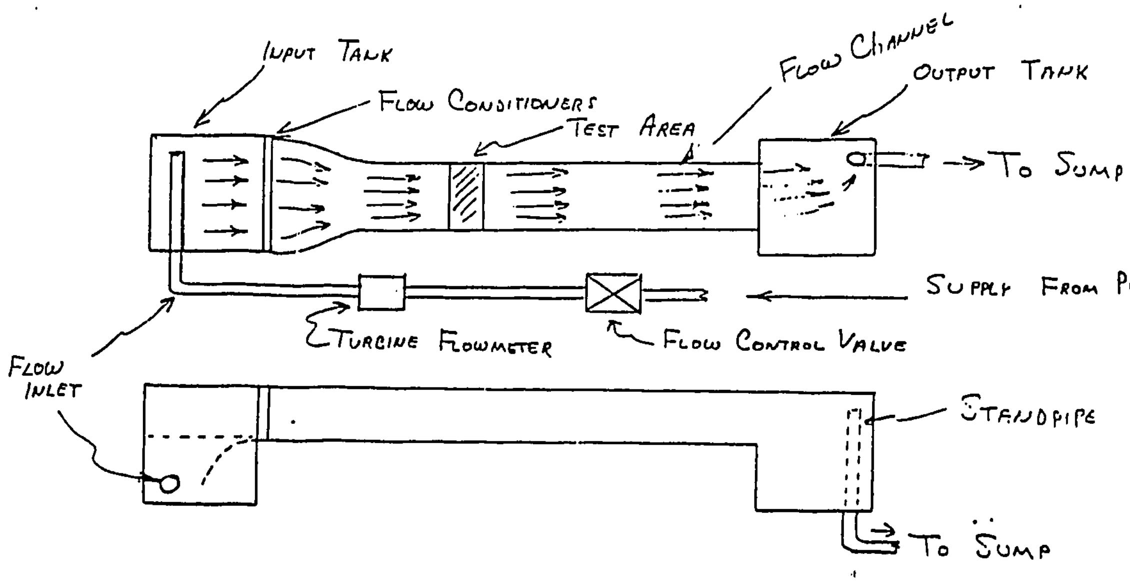
Input Tank
Flow Conditioners
Test Area
Flow Channel
Output Tank
To Sump
Supply From Pump
Turbine Flowmeter
Flow Control Valve
Flow Inlet
Standpipe
To Sump

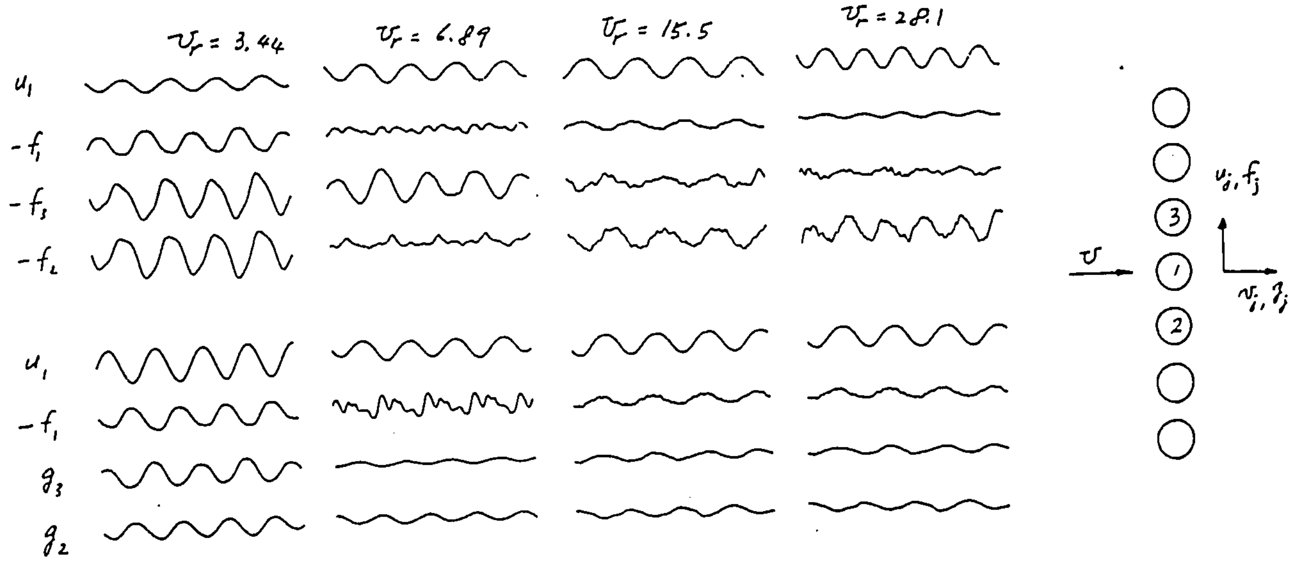
$v_r = 3.44$
$v_r = 6.89$
$v_r = 15.5$
$v_r = 28.1$
u_1
$-f_1$
$-f_3$
$-f_2$
u_1
$-f_1$
g_3
g_2
v
3
1
2
u_j, f_j
v_j, g_j

200

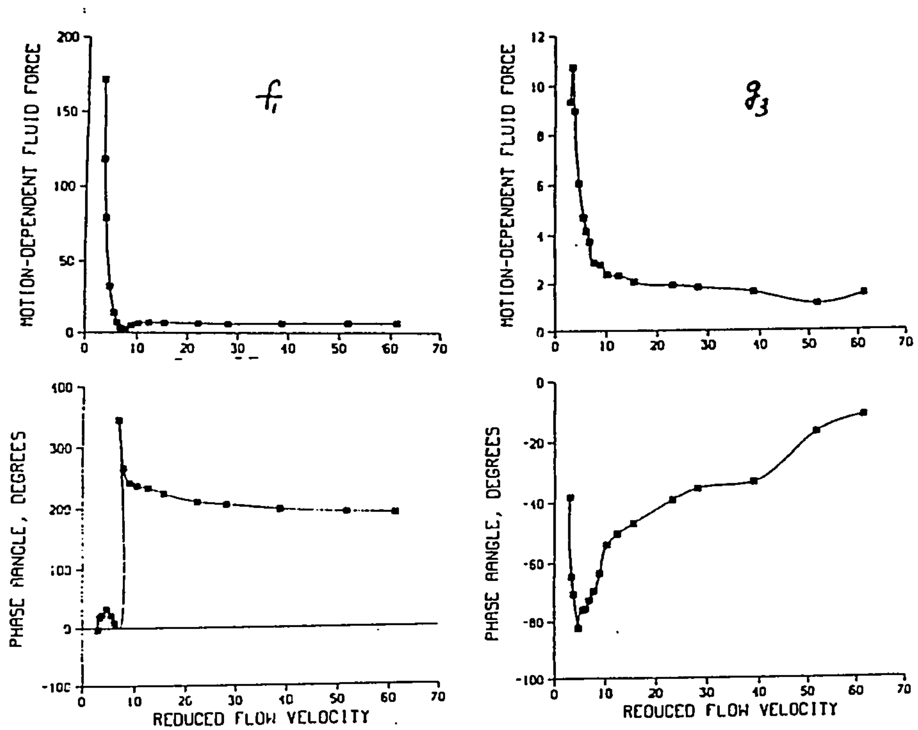

MOTION-DEPENDENT FLUID FORCE
f_1
g_3
PHASE ANGLE, DEGREES
REDUCED FLOW VELOCITY

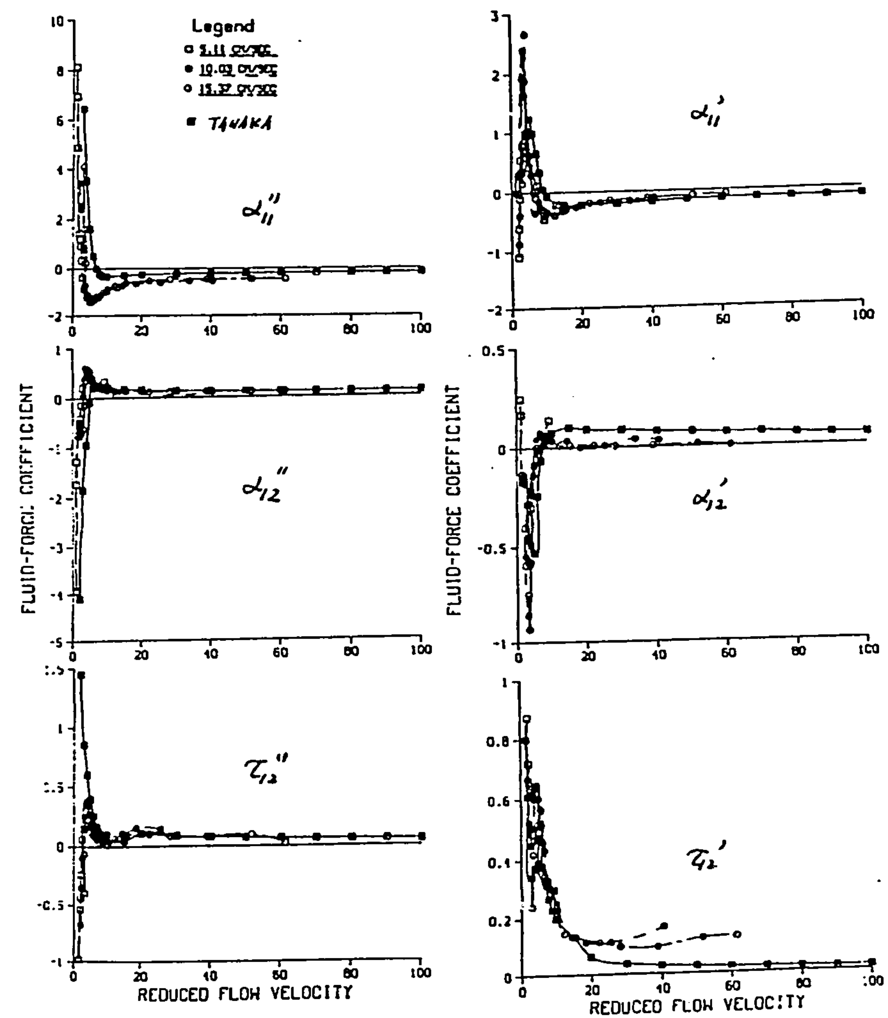

Legend
5.11 CY/SEC
10.03 CY/SEC
15.37 CY/SEC
TANAKA
α_{11}''
α_{11}'
α_{12}''
α_{12}'
τ_{12}''
τ_{12}'
FLUID-FORCE COEFFICIENT
REDUCED FLOW VELOCITY

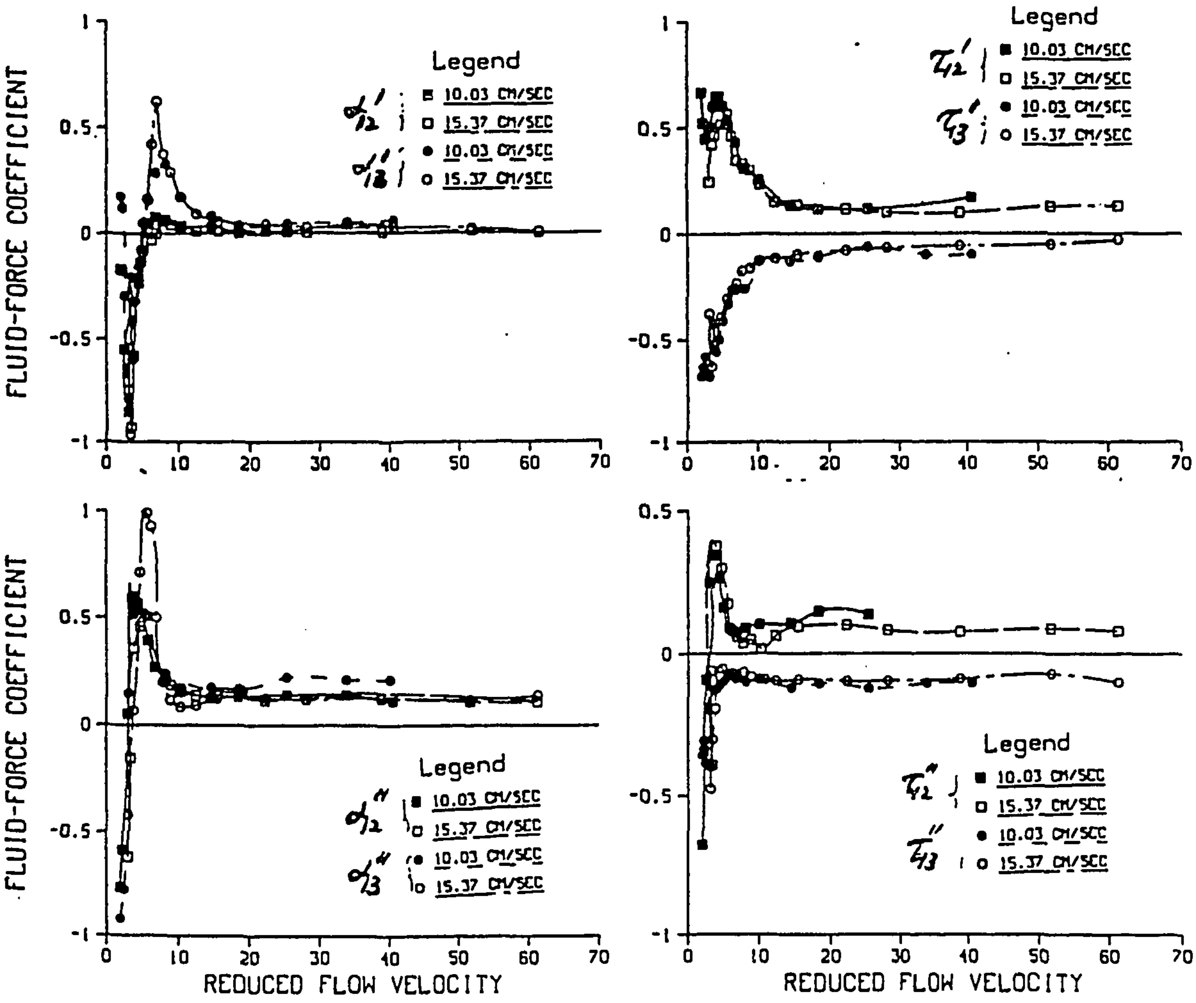
FLUID-FORCE COEFFICIENT
Legend
10.03 CM/SEC
15.37 CM/SEC
10.03 CM/SEC
15.37 CM/SEC
REDUCED FLOW VELOCITY
0
10
20
30
40
50
60
70
1
0.5
0
-0.5
-1

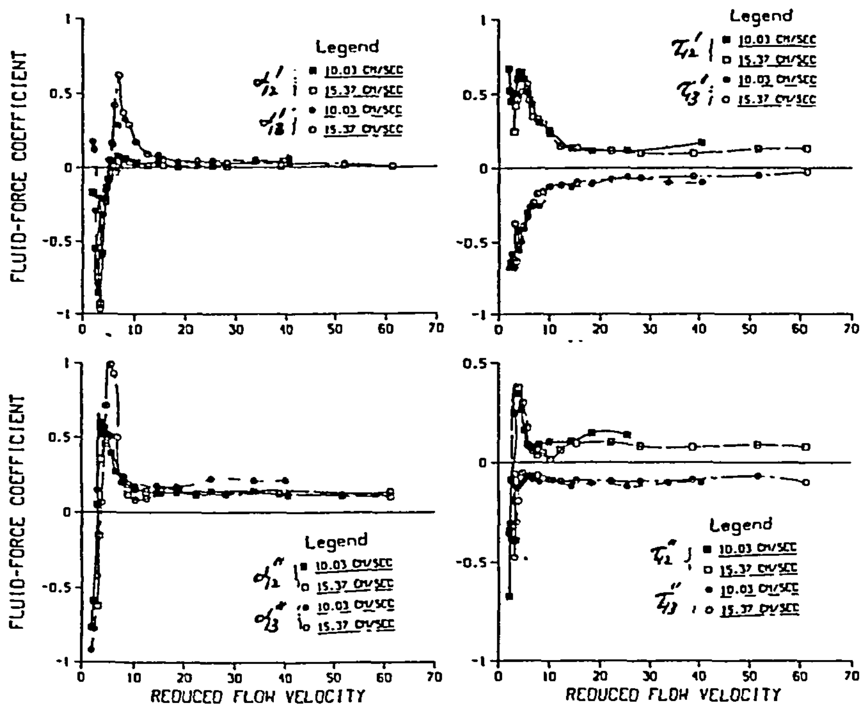
FLUID-FORCE COEFFICIENT
REDUCED FLOW VELOCITY
Legend
10.03 CM/SEC
15.37 CM/SEC
10.03 CM/SEC
15.37 CM/SEC